



## Article

# The Impact of Different Self-Selected Walking Speeds on Muscle Synergies in Transfemoral Amputees during Transient-State Gait

Pouyan Mehryar <sup>1,2,\*</sup>, Mohammad Shourijeh <sup>3</sup>, Tahmineh Rezaeian <sup>4</sup>, Aminreza Khandan <sup>5</sup>, Neil Messenger <sup>4</sup>, Rory O'Connor <sup>6</sup>, Farzam Farahmand <sup>5</sup> and Abbas Dehghani-Sanij <sup>2</sup>

<sup>1</sup> Department of Mechanical Engineering, Imperial College, London SW7 2AZ, UK

<sup>2</sup> School of Mechanical Engineering, University of Leeds, Leeds LS2 9JT, UK; a.a.dehghani-sanij@leeds.ac.uk

<sup>3</sup> Department of Mechanical Engineering, Rice University, Houston, TX 77005, USA

<sup>4</sup> School of Biomedical Sciences, Faculty of Biological Sciences, University of Leeds, Leeds LS2 9JT, UK; t.rezaeian@gmail.com (T.R.); neil\_messenger@ntlworld.com (N.M.)

<sup>5</sup> Faculty of Mechanical Engineering, Sharif University of Technology, Tehran P.O. Box 11155-9567, Iran; aminrezakhandan@gmail.com (A.K.); farahmand@sharif.edu (F.F.)

<sup>6</sup> School of Medicine, Faculty of Medicine and Health, University of Leeds, Leeds LS2 9JT, UK; r.j.o'connor@leeds.ac.uk

\* Correspondence: pmehryar@ic.ac.uk

**Abstract:** Facing above-knee amputation poses a significant hurdle due to its profound impact on walking ability. To overcome this challenge, a complex adaptation strategy is necessary at the neuromuscular level to facilitate safe movement with a prosthesis. Prior research conducted on lower-limb amputees has shown a comparable amount of intricacy exhibited by the neurological system, regardless of the level of amputation and state of walking. This research investigated the differences in muscle synergies among individuals with unilateral transfemoral amputations during walking at three different speeds of transient-state gait. Surface electromyography was recorded from eleven male transfemoral amputees' intact limbs (TFA), and the concatenated non-negative matrix factorization technique was used to identify muscle synergy components, synergy vectors (S), and activation coefficient profiles (C). Results showed varying levels of correlation across paired-speed comparisons in TFA, categorized as poor (S1), moderate (S3 and S4), and strong (S2). Statistically significant differences were observed in all activation coefficients except C3, particularly during the stance phase. This study can assist therapists in understanding muscle coordination in TFA during unsteady gait, contributing to rehabilitation programs for balance and mobility improvement, and designing myoelectric prosthetic systems to enhance their responsiveness to trips or falls.

**Keywords:** transfemoral amputee; surface electromyography; muscle synergy; concatenated non-negative matrix factorization; statistical parametric mapping



**Citation:** Mehryar, P.; Shourijeh, M.; Rezaeian, T.; Khandan, A.; Messenger, N.; O'Connor, R.; Farahmand, F.; Dehghani-Sanij, A. The Impact of Different Self-Selected Walking Speeds on Muscle Synergies in Transfemoral Amputees during Transient-State Gait. *Biomechanics* **2024**, *4*, 14–33. <https://doi.org/10.3390/biomechanics4010002>

Academic Editor: Pantelis T. Nikolaidis

Received: 22 October 2023

Revised: 16 December 2023

Accepted: 21 December 2023

Published: 11 January 2024



**Copyright:** © 2024 by the authors. Licensee MDPI, Basel, Switzerland. This article is an open access article distributed under the terms and conditions of the Creative Commons Attribution (CC BY) license (<https://creativecommons.org/licenses/by/4.0/>).

## 1. Introduction

Muscle synergies refer to the coordinated activation of groups of muscles to perform a particular movement. In healthy individuals, muscle synergies are well-coordinated and lead to efficient movement [1,2]. However, in individuals with limb amputations, the loss of a limb can significantly affect the coordination of muscle activation [3]. Transfemoral amputees (TFA), in particular, face challenges in achieving a smooth and coordinated gait due to the absence of the knee and ankle joints, which has an effect on the intact limb (IL) [4].

Transfemoral amputees rely on prosthetic devices to walk, which can cause significant changes in their gait patterns. These changes can lead to abnormal activation patterns of the intact and residual muscles, which can further affect the coordination of muscle synergies during walking [5,6]. Therefore, understanding the changes in muscle coordination from high and low levels, i.e., muscle activations and synergies in transfemoral amputees' intact

limbs, can provide insights into the underlying mechanisms of gait impairment in this population and potentially help therapists improve the quality of movement of amputees. In addition, this study of muscle coordination may yield important information for the creation of advanced prostheses.

While most studies on walking patterns focus on consistent, steady-state walking, it is also important to understand other states of gait in amputees, including gait initiation, the transient-state between gait initiation and steady-state walking, and the transition back to upright standing [3,5,7,8].

When transitioning from standing to walking, the body goes through a transient-state where the gait pattern is not yet fully established. During this phase, the body's muscles must work together to maintain balance and control movement. Recent studies have shown that the speed at which a person walks during this transient-state can have a significant impact on muscle coordination patterns [2,3,5]. Specifically, slower walking speeds have been shown to require greater muscle activation and recruitment to maintain stability and balance. This highlights the importance of understanding the effects of walking speeds during the transient-state on muscle coordination, particularly in populations with compromised gait patterns such as older adults, individuals with neurological disorders or lower limb amputees, as this may result in falls [9–11].

### *1.1. Muscle Synergy Analysis at Different Speeds*

Several studies showed that muscle synergies are shared and basic activation coefficient profiles held stable and consistent during steady-state walking over a wide range of speeds [12–14]. That is to say, the central nervous system (CNS) implements the same groups of muscle synergies, proportionally increasing the intensity of the activation coefficient profiles to satisfy the kinematic and kinetic demands of increased steady-state walking speed. In addition, other studies showed the shape and pattern of the four to six activation coefficient profiles have been impacted very little by changes in walking direction [15], locomotion mode [1,12,15–17], and loading and unloading of the body [18,19]. The similarity of the average activation coefficient profiles suggests each temporal component is shaped with respect to the total duration of the stride so that the resulting muscle activation has a long duration at low speeds and a short duration at high speeds [20]. However, some studies showed muscle synergies dependent on locomotion mode and speed. Kibushi et al. [21] concluded that the activation coefficient is flexibly controlled by the CNS in the regulation of walking speed. Yokoyama et al. [22] reported that different sets of muscle synergies were extracted depending on the task and speed. Other researchers reported that the timing and weighting of the patterns might significantly differ with changes in walking direction, speed, and loading and unloading of the body [18,19].

### *1.2. Muscle Synergy in the Pathological Population*

There have been studies focusing on pathological populations that show the number of muscle synergy groups is lower in people with Parkinson's disease, cerebral palsy, stroke, and spinal cord injuries than in normal subjects [13,23–28], suggesting a lower complexity in motor control. Clark et al. [13] showed two of the muscle synergies in healthy subjects might be merged in post-stroke patients during steady-state walking. This merging of muscle synergies was observed in incomplete spinal cord injury [28], Parkinson's disease [23], the upper extremity [27], and the lower extremity of stroke patients [26]. However, two studies have found no difference in the number of modules between healthy subjects and post-stroke patients [29,30]. The contradiction in the results of these studies could be due to the methodology, analysis, number and choice of muscles included, locomotion performed, chronicity of pathology, and heterogeneity of deficits inherently present following stroke.

### *1.3. Muscle Synergy in Lower Limb Amputees*

In prior studies, muscle synergy analysis was implemented to investigate the motor modules of a transtibial amputee during steady-state walking [31], ramp ascending [32],

and ramp descending [33], as well as transfemoral amputees during self-selected normal-speed steady-state and transient-state walking [5,6]. The same number of muscle synergies were found between the lower limb amputees and healthy subjects, indicating analogous complexity implemented by the CNS, which does not depend on the level of amputation. In addition, these studies found the activation coefficient was significantly different at some regions of the gait cycle (GC) by means of statistical parametric mapping [31,32]. However, the main limitation of these studies was that they only accounted for self-selected normal speed steady-state and transient-state walking.

#### *1.4. Aims and Objectives*

This study aimed to record the muscle activities of individuals with unilateral transfemoral amputations in their intact lower limbs while walking at three distinct, self-selected transient-state speeds. The utilization of muscle synergy analysis served as a method of decomposition in order to evaluate the disparities among the synergy components of TFA at varying velocities. The primary hypothesis was that there would exist certain muscle coordination patterns that are frequently necessary for the task, along with distinct patterns that signify the biomechanical requirements and adaptations resulting from speed change.

## **2. Materials and Methods**

### *2.1. Subjects*

This study involved eleven male volunteers who had undergone unilateral transfemoral amputation, with an average age of 55 years (SD = 8), a weight of 78 kg (SD = 15.3), and a height of 170.9 cm (SD = 7.9). The cause of amputation for all participants was trauma, with five cases related to war. The time elapsed since amputation was over 20 years for ten participants and 18 years for one, with a mean duration of 34.45 (SD = 7.61) years. All participants experienced amputation before the age of 30, with a mean age of 21.82 (SD = 4.83) years. Prior to the experiment, all subjects provided written, informed consent. The ethical review boards at the Djavad Mowafaghian Research Centre of Intelligent Neuro-Rehabilitation Technologies in Tehran, Iran, and the University of Leeds in the UK approved the experimental protocol.

### *2.2. Experimental Protocol*

The participants were asked to walk at three self-selected speeds: comfortable (normal), slow, and fast, according to their own perception. It means a slow or fast speed has been defined by the participants according to their comfortable speed. Initially, they walked along the path several times at their comfortable speed without any data recording, allowing them to become familiar with the tests and identify the starting point to ensure both feet hit the force platforms cleanly. The next gait cycle after gait initiation of leading or trailing limbs was considered such that the gait would still be in a transient state [8,9,21,34]. At least three walking trials for each participant were included at each speed.

### *2.3. Data Collection*

Ten muscles in the TFA intact limb were recorded using Myon wireless surface EMG (Myon AG, Schwarzenberg, Switzerland), disposable, self-adhesive Ag/AgCl dual snap electrodes with a 20 mm center-to-center distance. The Rectus femoris (RF) and vasti (vastus medialis (VM) and vastus lateralis (VL)), biceps femoris long head (BFLH), semitendinosus (SEM), tensor fascia latae (TFL), tibialis anterior (TA), and triceps surae (gastrocnemius medialis (GM), gastrocnemius lateralis (GL), and soleus (SOL)) activity were captured following the Stegman and Mermans' guide for locating muscle bellies [35]. The participants were asked to walk at their slow and fast speeds after data on comfortable walking speeds had been gathered.

A 6-camera motion analysis system (Vicon Motion Systems, Oxford, UK) and two 40 cm · 60 cm and 80 cm · 60 cm Kistler force platforms embedded in the floor were synchronized with Wireless Myon Surface EMG. Fourteen mm spherical passive reflective

markers were fixed on the skin of anatomical landmarks to define body segments for later kinematical analysis (Figure 1). Marker tracking was performed using Nexus 2.5 (Vicon Motion Systems, Oxford, UK). A 12-segment body model was created by using the markers for 3D coordination in Visual 3D 5v. Visual 3D provides the kinematics of each segment, including its center of mass (COM) position and its speed during any movement. The walking speed of the TFA was determined to be  $0.61 \pm 0.09$  m/s (slow),  $0.76 \pm 0.16$  m/s (normal), and  $0.97 \pm 0.14$  m/s (fast) (see Supplementary Material for probability distributions of walking speeds).

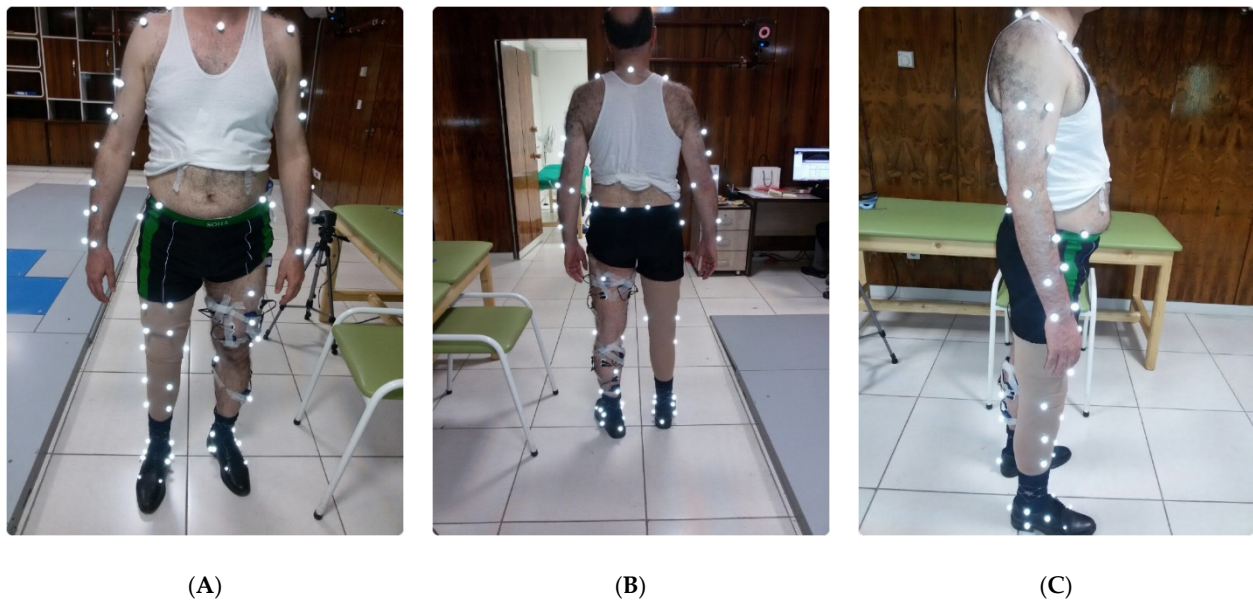


**Figure 1.** EMG and reflective marker attachments on TFA (A) front, (B) back, and (C) side view.

#### 2.4. Processing Surface EMG and Preparation for Muscle Synergy Analysis

The analytical work was implemented in MATLAB R2017 (Mathworks, Inc., Natick, MA, USA). The GCs segmentation was determined by analyzing the trajectories of reflective markers located on the foot's instrumented parts, namely the calcaneus and the first metatarsal. This analysis was carried out after the foot made contact with the force platform. The surface EMG signals were processed by first demeaning them, then applying a fourth-order Butterworth bandpass filter with a cut-off frequency of 20–500 Hz. Next, the signals were full-wave rectified and low-pass filtered using a zero-lag 2nd-order Butterworth filter at 6 Hz. Finally, the signals were normalized in amplitude with respect to the highest peak observed across all trials and walking speeds and then time-normalized to generate 101 data points for each GC [36–39].

#### 2.5. Concatenated Non-Negative Matrix Factorization (CNMF) Frameworks

We extracted motor modules using a concatenated non-negative matrix factorization (CNMF) algorithm for each speed separately [2,40]. In this technique,  $A^C$  is an n-by-m ( $n$  = number of subjects  $\times$  number of gait cycles  $\times$  101 and  $m$  = number of muscles) and  $C^C$  is an n-by-k ( $k$  = number of synergy groups), which are concatenated, whereas  $S$  is a k-by-m (fixed synergy) [31,32,40]. The objective function of CNMF is as follows: Equation (1)

$$J = \sum_{i=1}^{N_s} \frac{\|A_i^C - C_i^C S\|_F}{\|A_i^C\|_F} \quad (1)$$

where  $\|A_i^C\|_F$  represents the Frobenius norm of a vector defined as  $\sqrt{\text{tr}(AA^T)}$  ( $\text{tr}$  = matrix trace and  $A^T$  = matrix  $A$  conjugate transpose),  $C_i^C$  is a concatenated coefficient,  $S$  is a fixed synergy vector, and  $N_s$  is the number of subjects. In this paper, CNMF has been

implemented due to an a priori hypothesis that accounts for the similarities in a population, which can be considered a model of a variation of homogeneous people rather than an individual.

### 2.6. CNMF MATLAB Implementation

Random values of  $C$  and  $S$  were chosen (rand function in MATLAB) in order to initiate the CNMF. An alternating least squares algorithm was used to attain optimal  $C$  and  $S$ . These values must satisfy the Frobenius norm to minimize the error  $\|A_i^c - C_i^c S\|_F$ . Norm 2 of each  $S_i$  was normalized to 1 to avoid the indeterminacy of matrix factorization. To ensure reliability, perturbations were introduced to the data. In order to find the final optimal solution for  $S$  and  $C$ , three iterations were performed for the whole framework. However, the perturbation was not applied in the last iteration [32,40]. See [2,40] for more details.

### 2.7. Dimensionality (Variance Accounted for)

To reconstruct the original signal, the number of synergy groups must be identified. This is accomplished by examining the changes in total Variance Accounted For (VAF) as the number of muscle synergies is adjusted [36,38]. VAF was defined as the uncentered Pearson correlation coefficient between the original and reconstructed EMG data [41] in Equation (2). A high VAF criterion ensured that each muscle tuning curve would be precisely reconstructed, thereby enabling the muscle synergies to effectively elucidate the essential spatiotemporal properties of each muscle activation pattern.

$$\text{VAF}^c = (1 - \sum_{o=1}^n \sum_{p=1}^m e_{op}^2 / \sum_{o=1}^n \sum_{p=1}^m A_{op}^2) \times 100 \quad (2)$$

where the indices  $o$  and  $p$  stand for the rows and columns of the quantities  $e$  and  $A$ , and  $e$  is the error, or A-CS. A VAF value greater than 0.80 is considered the minimum threshold for determining the appropriate number, unless an additional factor increases the VAF by less than 0.05 [42]. The standard for evaluating the quality of muscle reconstruction was established using the intra-class correlation coefficient (ICC) test, with a value greater than 0.5 being considered the minimum threshold for each individual muscle [31,32].

### 2.8. Synergy Output Normalization

The process involved normalizing the activation coefficient profiles by setting their maximum values as the normalization factor. The muscle synergy vectors were then scaled using the inverse of the normalized activation coefficient profile. This standardized both the activation coefficient profile and muscle synergy vector, ensuring that they represented muscle recruitment and amplitude information within a range of 0 to 1. The goal was to capture temporal modulation in muscle recruitment and amplitude information using arbitrary units [42].

### 2.9. Between Population Synergy Sorting

In order to account for significant variations in data variability, a functional sorting technique were employed. This involved rearranging the indices of muscle synergy and the coefficient for a specific speed based on their relationship with other speeds. A reference point was chosen to sort the muscle synergy components, taking into account the similarity of  $S$  and/or  $C$  values using the maximum coefficient of determination ( $R^2$ ) metric. By rearranging the order of synergy components, it became possible to make statistical comparisons between different groups. In the study mentioned, the muscle synergy components for slow and fast speeds were sorted based on the muscle synergy components for the normal speed [38,43].

### 2.10. Statistical Analysis

The evaluation of similarity between the reconstructed and original signals for each muscle involved the calculation of the ICC value. ICC assessed the similarity in patterns.

Additionally, to assess the similarity of concatenated C values across trials or subjects, ICC(C,k) based on two-way mixed models with average measurements and no interactions was utilized. According to [44], ICC values below 0.5 indicated a low correlation, values between 0.5 and 0.75 indicated a moderate correlation, and values above 0.75 indicated a high correlation.

A comprehensive statistical evaluation of all activation coefficients was performed across the gait cycle to investigate the hypothesis regarding the entire time series rather than specific time points. This analysis utilized the MATLAB R2017 software and employed an ANOVA repeated measure based on the Statistical Parametric Mapping (SPM) approach [45].

### 3. Results

#### 3.1. Dimensionality

The VAF comparison was performed for each group between speeds. The group-muscle criterion is to select the lowest number of synergies that accounted for >80%, and the next synergy group will not increase VAF by more than 5%. Figure 2 shows the VAF of TFA during transient-state walking at different speeds. Three to seven synergy groups in slow and normal and two to seven in fast met the group-muscle criterion (>80%). However, four synergies were selected as the optimal number of groups based on the 5% criterion for all speeds.

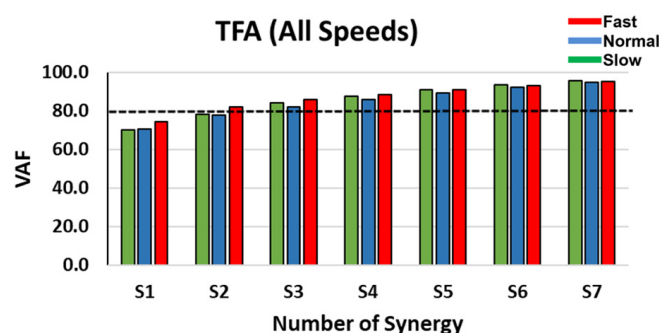


**Figure 2.** VAF comparison as a function of the number of synergies in TFA at slow, normal, and fast speeds.

#### 3.2. Intra-Class Correlation Coefficient (ICC)

ICC takes the signal pattern comparison into account and allows for multiple comparisons to be made. ICC was used for two purposes in this study: (1) to assess the similarities between reconstructed and original muscle EMG signal (within-subject and between-subject for individual-muscle criterion); and (2) to evaluate the repeatability of coefficients between trials/subjects.

Figure 3 shows a correlation between the reconstructed and the original individual muscle signals in TFA at three different speeds. All muscles within their respective speeds showed a moderate to high correlation.

#### 3.3. Inter-Subject Variability of C

As shown in Table 1, high repeatability (ICC > 0.75) was perceived as the ICC value for between trials/subjects similarities in each speed category was above 0.80 except in TFA C4 normal speed. The ICC for TFA C4 showed 0.29, indicating poor repeatability (ICC < 0.5).

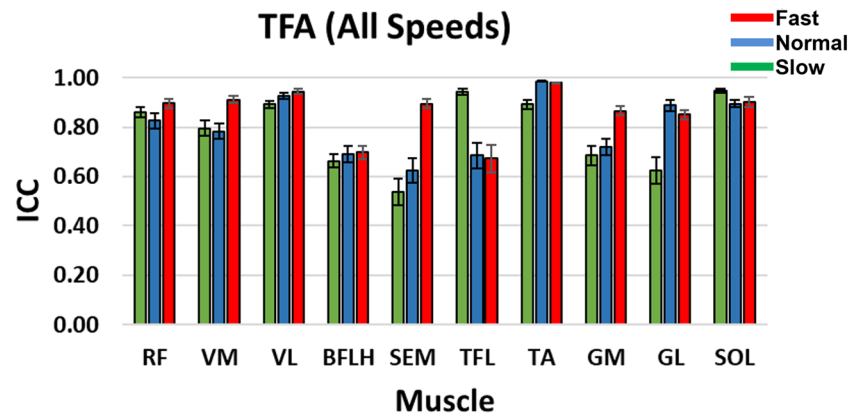


**Figure 3.** TFA ICC between the reconstructed and original muscle signal when four synergy groups were selected during slow, normal, and fast speeds. Standard error bars indicate  $\pm$  one.

**Table 1.** TFA activation coefficient profiles (C1–C4) repeatability between trials/subjects using ICC.

	TFA Intra-Class Correlation Coefficient			
	C1	C2	C3	C4
Slow	0.89	0.80	0.97	0.87
Normal	0.98	0.94	0.90	0.29
Fast	0.98	0.97	0.94	0.85

### 3.4. TFA Muscle Synergy Description

TFA S1 was related to the recruitment of TFL in slow (during early stance (ES) and terminal swing (TSW)), SOL and TFL in normal (during ES-midstance (MS), terminal stance (TS), and TSW), and knee extensors in fast walking (during ES-MS) across speeds (Table 2). TFA S2 related to body support and forward propulsion, in which the plantarflexor muscles were primarily involved across speeds (Table 3). TFA S3 was related to the activation of the knee extensors during ES and TSW of slow and normal walking and SEM and VL during ES and MS-TSW of fast walking (Table 4). TFA S4 related to the leg swing as well as the transition from swing to stance, in which the dorsiflexor muscle was primarily involved across speeds (Table 5). The TFA muscle synergy description is based on Figure 4A,B.

**Table 2.** TFA muscle weighting contribution and corresponding activation timing profile of S1 across speeds. Abbreviations: Rectus femoris (RF) and vasti (vastus medialis (VM) and vastus lateralis (VL)), biceps femoris long head (BFLH), semitendinosus (SEM), tensor fascia latae (TFL), tibialis anterior (TA), and triceps surae (gastrocnemius medialis (GM), gastrocnemius lateralis (GL), and soleus (SOL)). Initial contact (IC), loading response (LR), early stance (ES, i.e., (IC-LR)), midstance (MS), terminal stance (TS), initial swing (ISW), midswing (MSW), and terminal swing (TSW).

TFA Synergy 1 (All Speeds)			
Module	Muscle		Activation
	Primary (>0.5) *	Secondary (<0.5) *	
Fast	VM, RF, VL	TFL, BFLH, SOL, GM	ES, TSW
Normal	SOL, TFL	GM, BFLH, VM, RF, VL	ES-MS, TS, TSW
Slow	TFL	TA, VL, SOL, RF, GM, SEM	IC-LR, MS

\* Muscle weighting: primary > 0.5 and secondary < 0.5.

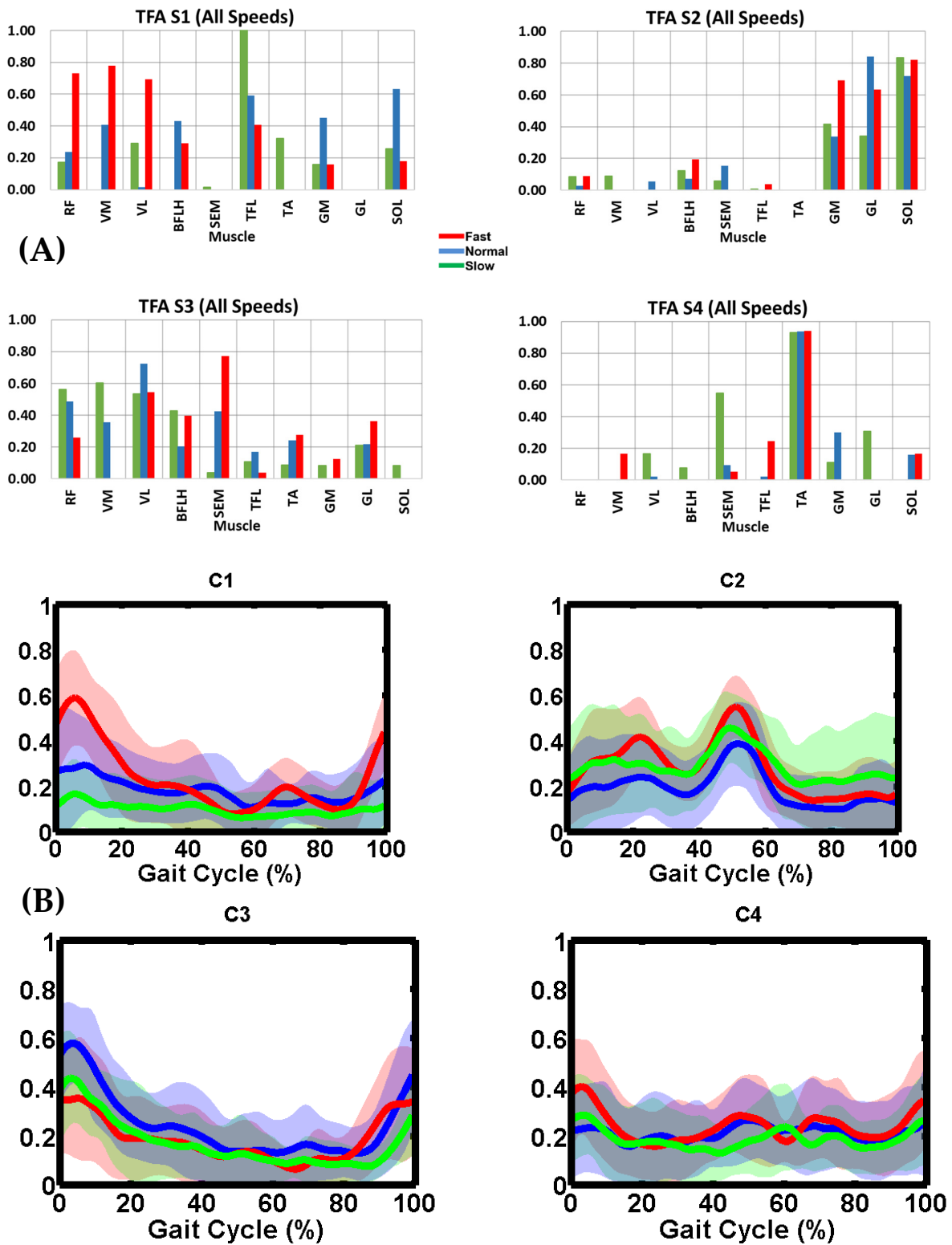


**Figure 4.** TFA (A) muscle synergy vectors (S1–S4) and (B) activation coefficient profiles (C1–C4) during slow, normal, and fast speeds. In (A), the bars represent muscle weightings within each synergy group. In (B), the thick lines represent the mean trajectory of activation coefficient profiles, and the shaded area is  $\pm$  one standard deviation from the mean. TFA slow speed was  $0.61 \pm 0.09$  m/s (stance:  $73.4 \pm 3.1\%$  and swing:  $26.6 \pm 3.1\%$ ). TFA normal speed was  $0.76 \pm 0.16$  m/s (stance:  $70.8 \pm 3.6\%$  and swing:  $29.2 \pm 3.6\%$ ). TFA fast speed was  $0.97 \pm 0.14$  m/s (stance:  $69.8 \pm 2.6\%$  and swing:  $30.2 \pm 2.6\%$ ). Slow, normal, and fast illustrated in green, blue and red, respectively.

**Table 3.** TFA muscle weighting contribution and corresponding activation timing profile of S2 across speeds (Refer to Table 2 for abbreviations).

TFA Synergy 2 (All Speeds)			
Module	Muscle		Activation
	Primary (>0.5)	Secondary (<0.5)	
Fast	SOL, GM, GL	BFLH, RF, TFL	MS, TS
Normal	GL, SOL	GM, SEM, BFLH, VL, RF	MS, TS
Slow	SOL	GM, GL, BFLH, RF, VM, SEM	MS, TS

**Table 4.** TFA muscle weighting contribution and corresponding activation timing profile of S3 across speeds (Refer to Table 2 for abbreviations).

TFA Synergy 3 (All Speeds)			
Module	Muscle		Activation
	Primary (>0.5)	Secondary (<0.5)	
Fast	SEM, VL	BFLH, GL, TA, RF, GM, TFL	ES, MSW-TSW
Normal	VL	RF, SEM, VM, TA, GL, BFLH, TFL	IC-LR, TSW
Slow	VM, RF, VL	BFLH, GL, TFL, TA, GM, SOL, SEM	IC-LR, TSW

**Table 5.** TFA muscle weighting contribution and corresponding activation timing profile of S4 across speeds (Refer to Table 2 for abbreviations).

TFA Synergy 4 (All Speeds)			
Module	Muscle		Activation
	Primary (>0.5)	Secondary (<0.5)	
Fast	TA	TFL, VM, SOL, SEM	IC-LR, TS, ISW, TSW
Normal	TA	GM, SOL, SEM, VL, TFL	IC-LR, TS-PSW-ISW, TSW
Slow	TA, SEM	GL, VL, GM, BFLH	IC-LR, PSW-ISW, TSW

### 3.5. Synergy Vector Comparison

As shown in Table 6, TFA normal-slow  $R^2$  showed a low correlation with S1, a moderate correlation with S4, and a strong correlation with S2 and S3. The comparison between the modules of normal and fast illustrated low (S1), moderate (S3), and strong (S2 and S4) correlations. The correlation between TFA fast-slow  $R^2$  revealed a low (S1 and S3), moderate (S4), and strong (S2) relationship between muscle synergies. The module average goodness of fit for each muscle synergy across speeds illustrated a low correlation for S1 (0.04), a moderate correlation for S3 (0.53) and S4 (0.65), as well as a strong correlation for S2 (0.83). Overall average  $R^2$  of all four modules combined (S1–S4) showed low correlation between fast-slow ( $R^2_{Average} = 0.40$ ) and moderate correlation between normal-slow ( $R^2_{Average} = 0.53$ ) and normal-fast ( $R^2_{Average} = 0.61$ ) gait.

**Table 6.**  $R^2$  values for four muscle synergies (S1–S4) in TFA at different speeds; the module average obtained column-wise represents the average correlation of each module with respect to all paired-wise speed comparisons. The overall average value obtained row-wise represents the average correlation of all muscle synergies with respect to each pair-wise speed comparison.

	S1	S2	S3	S4	Overall Average
Normal vs. Slow	0	0.78	0.72	0.61	0.53
Normal vs. Fast	0.13	0.83	0.66	0.83	0.61
Fast vs. Slow	0	0.89	0.2	0.5	0.40
Module Average	0.04	0.83	0.53	0.65	

### 3.6. Activation Coefficient Profile Comparison

A priori hypothesis was to investigate the effect of speeds on individual activation coefficient profiles during gait. Therefore, a one-way repeated-measures ANOVA (represented as a black trajectory in Figure 5) was implemented to investigate the within-subject F statistics. It is worth mentioning that a one-way ANOVA was performed between-subjects for demonstration (represented as a red trajectory in (Figure 5); however, this is not an appropriate test since the same subjects performed transient-state walking at different speeds. Moreover, the between-subject analysis yields a small F value because between-subject variability is large relative to between-condition variability. The within-subject analysis yields a large F value because paired effects are large relative to paired variability. Post hoc analysis was carried out to further investigate the differences between speeds. Multiple post hoc paired or two sample *t*-tests increase the chances of making a type I error (false positive). Therefore, alpha was corrected according to the number of comparisons made to decrease the likelihood of a type I error, increase the critical threshold, and ensure the false positive error rate was appropriate for the number of comparisons made. In this case, a Bonferroni threshold of  $p = 0.017$  was adopted for the three walking speeds to retain a family-wise error of  $\alpha = 0.05$ , which was then used for inference calculation.

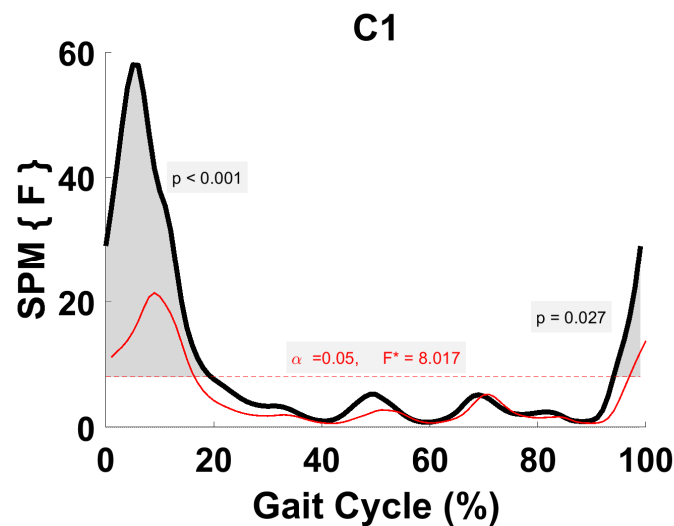


**Figure 5.** TFA C1 parametric RM ANOVA within- and between-subjects, depicting significant differences between speeds. The horizontal red dotted line indicates the critical threshold of 8.02. Suprathereshold clusters are shown in gray where  $p < 0.05$ . Black line is RM ANOVA (Within) and red line is ANOVA (Between).

As shown in Figure 5, the main SPM analysis found significant differences in TFA C1 between three different speeds. Two suprathereshold clusters were found at 0–19% ( $p = 0.0$ ) and 94–100% ( $p = 0.27$ ) GC. A post hoc paired *t*-test was conducted pairwise between speeds, which revealed C1 was significantly different between fast-normal at 0–8% ( $p = 0.001$ ) as well as fast-slow at 0–14% ( $p = 0.0$ ) and 95–100% ( $p = 0.014$ ) GC (Figure 6). As shown in Figure 7, SPM analysis revealed three suprathereshold clusters across speeds in C2 within-subject at 19% ( $p = 0.049$ ), 44–53% ( $p = 0.006$ ), and 68% (0.05). No significant differences were found between-subjects. A post hoc paired *t*-test showed a significant difference between fast-normal and 45–49% ( $p = 0.010$ ) GC (Figure 8). As shown in Figure 9, SPM analysis showed no significant difference in TFA C3 across speeds. As shown in Figure 10, SPM analysis showed a statistically significant difference in C4 within-subject across speeds. One suprathereshold cluster occurred at 42–47% ( $p = 0.014$ ). No significant differences were found between-subjects. A post hoc paired *t*-test showed a significant difference between fast-slow at 42–45% ( $p = 0.013$ ) GC (Figure 11).

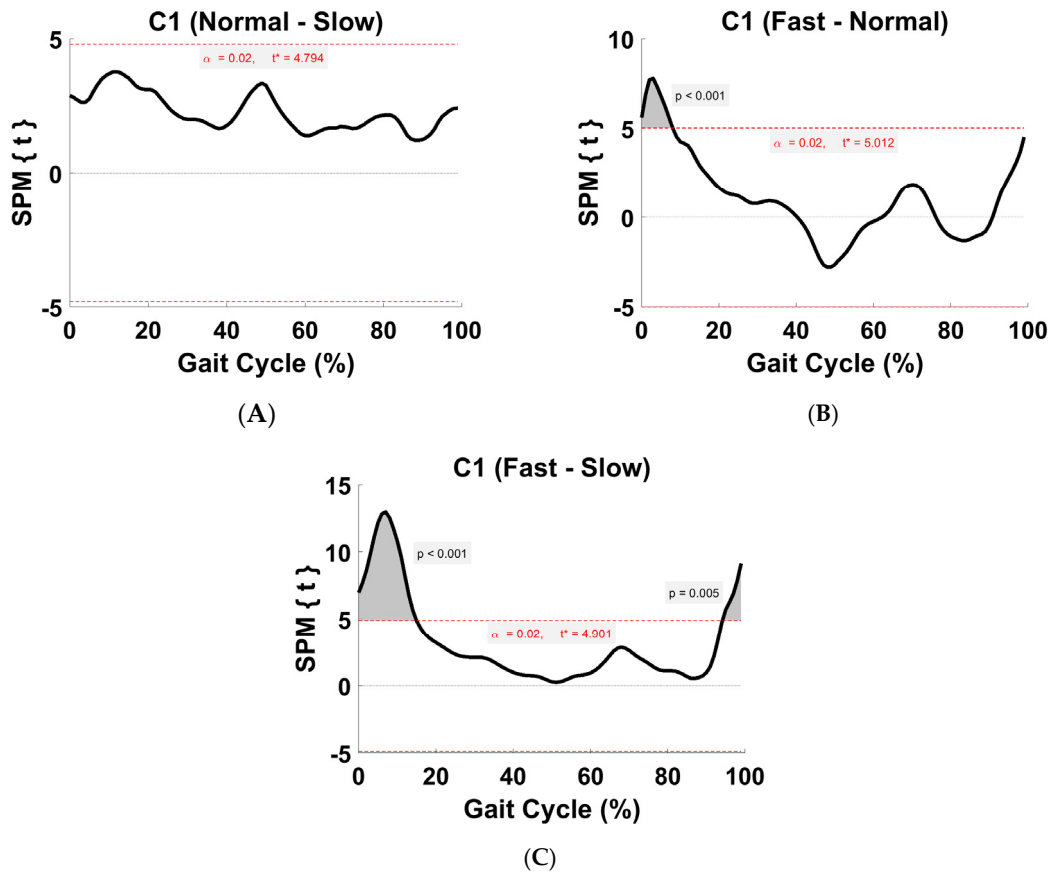


**Figure 6.** TFA C1 within-subject post hoc paired t statistic between pairs of walking speeds. The red dashed lines indicate critical thresholds of  $t^* = 4.79, 5.01,$  and  $4.9$  for (A–C), respectively. Suprathreshold clusters are shown in gray where  $p < 0.02$ .

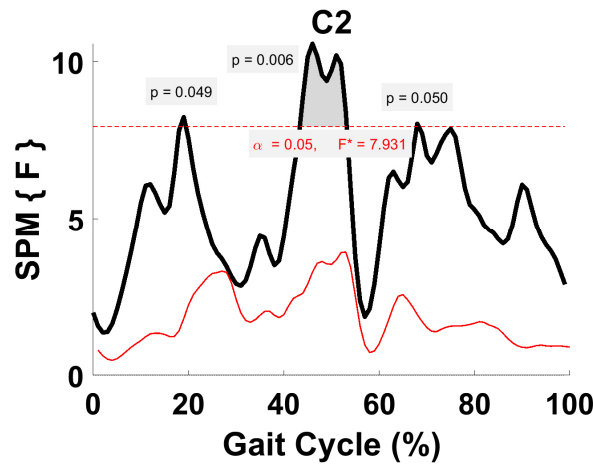


**Figure 7.** TFA C2 parametric RM ANOVA within- and between-subjects, depicting significant differences between speeds. The horizontal red dotted line indicates the critical threshold of  $7.93$ . Suprathreshold clusters are shown in gray where  $p < 0.05$ . Black line is RM ANOVA (Within) and red line is ANOVA (Between).

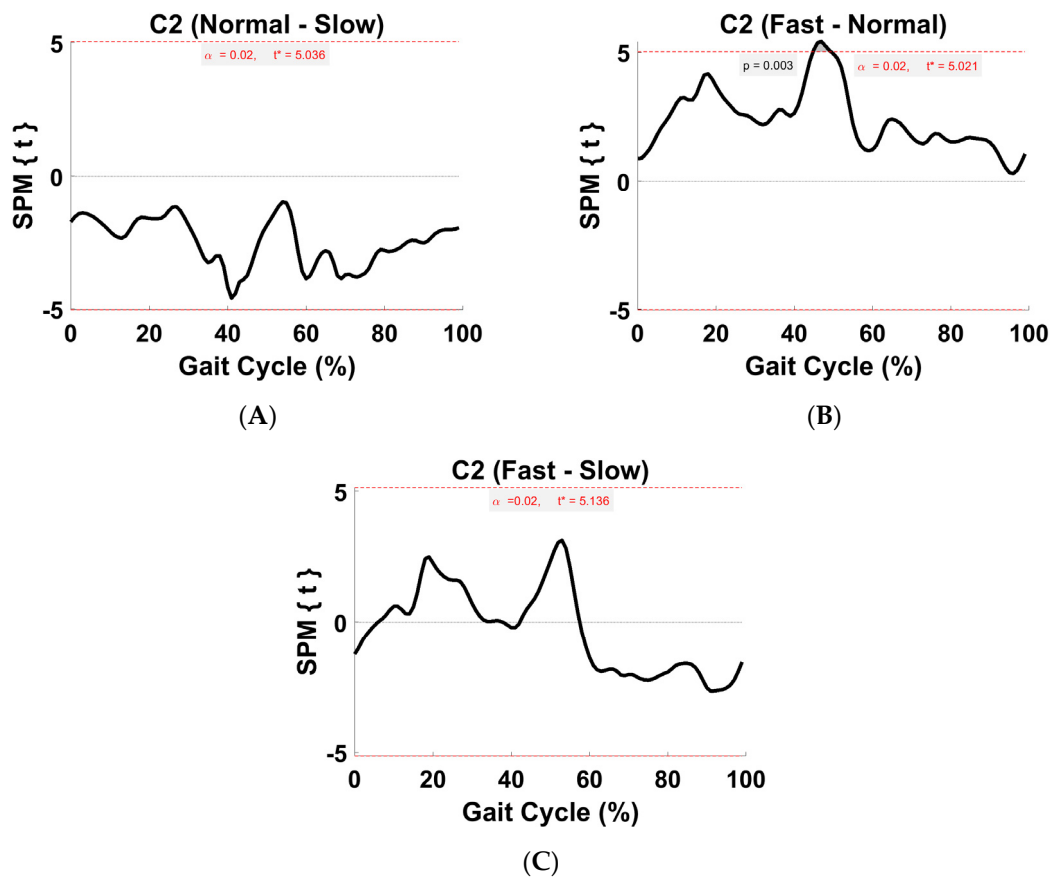


**Figure 8.** TFA C2 within-subject post hoc paired t statistic between pairs of walking speeds. The red dashed lines indicate critical thresholds of  $t^* = 5.04$ , 5.02, and 5.14 for (A–C), respectively. Suprathreshold clusters are shown in gray where  $p < 0.02$ .

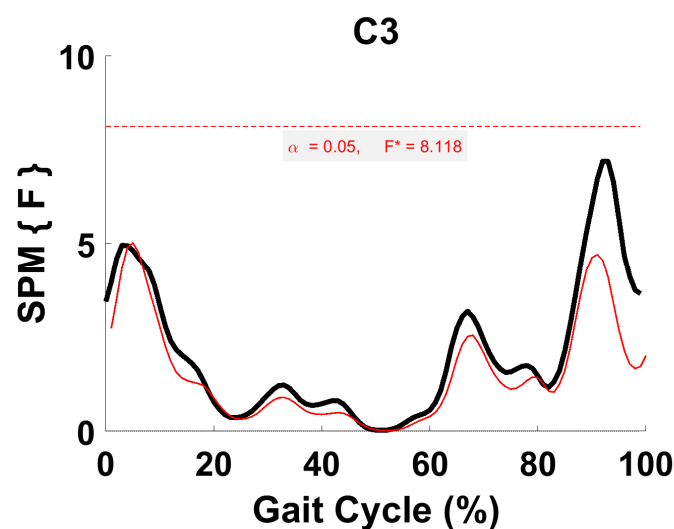


**Figure 9.** TFA C3 parametric RM ANOVA within- and between-subjects, depicting significant differences between speeds. The horizontal red dotted line indicates the critical threshold of 8.12. Suprathreshold clusters are shown in gray where  $p < 0.05$ . Black line is RM ANOVA (Within) and red line is ANOVA (Between).

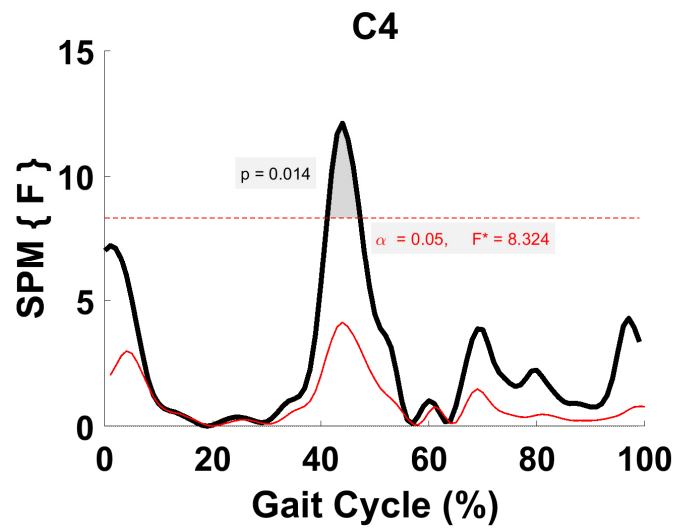


**Figure 10.** TFA C4 parametric RM ANOVA within- and between-subjects, depicting significant differences between speeds. The horizontal red dotted line indicates the critical threshold of 8.32. Suprathreshold clusters are shown in gray where  $p < 0.05$ . Black line is RM ANOVA (Within) and red line is ANOVA (Between).

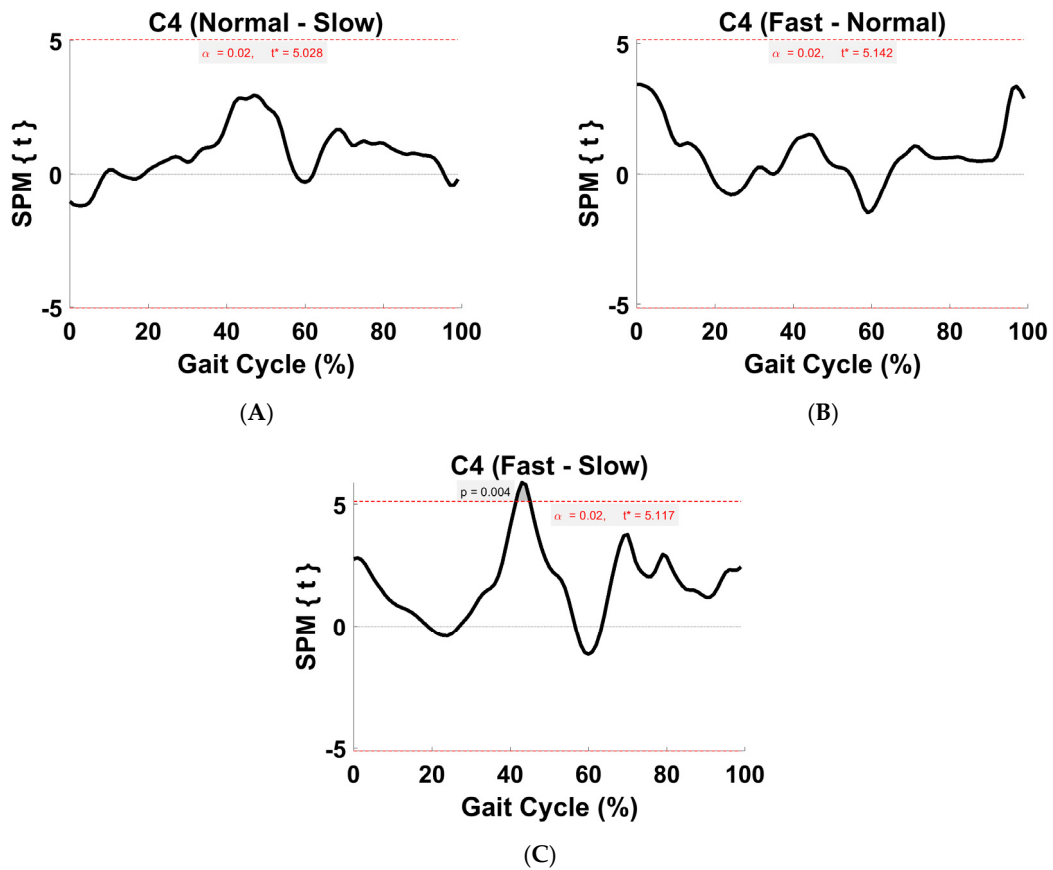


**Figure 11.** TFA C4 within-subject post hoc paired t statistic between pairs of walking speeds. The red dashed lines indicate critical thresholds of  $t^* = 5.03, 5.14,$  and  $5.12$  for (A–C), respectively. Suprathreshold clusters are shown in gray where  $p < 0.02$ .

## 4. Discussion

### 4.1. VAF

The number of muscle synergy groupings was determined according to the literature ( $k = 4$ ) [13,31,32,37,38,41,43]. Four modules were selected for the TFA in slow, normal, and fast transient-state walking, which accounted for a VAF of 88%, 86%, and 88%, respectively. A higher VAF using five synergies was obtained. However, four synergies were believed to provide more distinct synergistic groups of muscle EMG contents. Moreover, since the VAF value was higher than 80% and the difference between them was not more than 5%, four synergies were chosen for TFA.

The comparable number of modules suggests that the neurological system's complexity in muscle recruitment is similar in amputees at different transient-state walking speeds. The results of this study are consistent with prior research conducted on individuals with transtibial amputations [31,32] and transfemoral amputations during self-selected steady-state walking [6] in relation to the dimensionality of muscle synergy. These findings indicate that the neurological system maintains a consistent strategy, regardless of the specific level of amputation. The outcomes observed in individuals with TFAs and TTAs, with respect to synergistic strategies, exhibit disparities when compared to other patient cohorts, such as those recovering from stroke [13]. However, these outcomes demonstrate similarities with joint injury groups, specifically individuals with orthopaedic injury (anterior cruciate ligament deficiency) [39]. Hence, it seems that the complexity of neurological control, as measured by the number of recruited modules, is not influenced by the level of amputation or the gait state.

### 4.2. CNMF Activation Coefficient Profile Repeatability (ICC)

The ICC was also utilized to evaluate the consistency and similarity of activation coefficients between different trials and subjects. This step is crucial because CNMF fixes an unknown variable,  $S$ , while allowing variation in  $C$ . A strong correlation was observed in TFA across different speeds. However, TFA C4 exhibited poor consistency (with high variability between subjects), indicating differences in coefficient patterns between trials and subjects at normal speed. However, the ICC does not indicate which phase of variability is associated with this inconsistency. One possible explanation is that S4 consists of the primary activity of the TA muscle, which contributes to slowing down the leg during the early and late swing phases and facilitates foot clearance. Consequently, the instability in the TFA prosthetic leg (due to feelings of insecurity) during the weight acceptance phase before the opposite leg starts swinging may contribute to the inconsistency in the shape of C4 between trials and subjects. Moreover, due to the presence of the triceps surae muscle group during weight acceptance, the TA muscle co-contracts to stabilize the ankle joint, which could lead to discrepancies in TFA C4. Additionally, previous research has demonstrated considerable variability in TA muscle activity during walking among different individuals [46,47].

Finally, it is possible to provide a psychological explanation for this phenomenon. TFA individuals are accustomed to walking at a normal pace. However, walking at slower or faster speeds, particularly during transitional states, presents a challenging task for them. As a result, they become more cautious and adopt a careful walking pattern when walking at speeds other than their comfortable and self-selected normal pace. The increased cognitive load in these situations may lead to a reduction in variability in muscle activities [48].

### 4.3. Within-Subject Comparison (Synergy/Module/S)

Previous reports illustrated similarity in the construction of muscle synergies among non-amputees at different walking speeds during steady-state walking [12–14,37]. However, changes in muscle synergies between non-amputees and amputees have been illustrated at normal transient-state walking speeds [2,5]. Furthermore, Gui and Zhang [14] showed similar motor modules across speeds, with modest changes in the timing of

coefficients for the non-amputees to satisfy the kinematic and kinetic requirements of different steady-state walking speeds. However, others found that different muscle synergies are recruited as the result of a change in steady-state walking speeds and locomotion modes [18,19,22].

TFA  $R^2$  results revealed poor (S1), moderate (S3 and S4), and strong (S2) correlations across paired-speed comparisons (i.e., module average). The primary muscle weighing in S1 is different across speeds, which led to poor correlation. On the contrary, the analogous muscle group in S2 resulted in a strong correlation between speeds. The lowest correlation in S1 (0) and S3 (0.2) between fast-slow walking was due to the difference in weighting ratio (Table 6). The difference could be attributed to the significant change in speeds, which resulted in neuromuscular modulation at the transition from stance to swing phase and body support phase of the GC [14].

#### 4.4. Synergy Vector Comparison with Literature

Prior research showed four synergy groups in TFA during normal transient-state walking, which confirms the complexity of muscle coordination in TFA does not change as compared to non-amputee individuals during transient-state walking [5]. In addition, a study by [6] showed four muscle synergies in TFA during self-selected steady-state walking. In the present study, the muscle synergies extracted from TFA during slow transient-state walking match well with the four synergies in [6]. This is also in accordance with the previous studies on muscle synergies during gait [20,37].

In addition, a study carried out by [37] showed five muscle activation modules were sufficient to generate forward dynamics simulations of gait and their associations with biomechanical subtasks of walking. The study reported that knee and hip extensors contribute to weight acceptance and body support in early stance while acting to decelerate forward motion (Module 1), plantarflexors contribute to body weight support, loading, and propulsion in before toe off (Module 2), dorsiflexor and hip flexor muscles contribute to deceleration of the leg in the early and late swing as well as trunk stabilization throughout the swing phase (Module 3), knee flexors decelerate the leg in late swing (Module 4), and hip flexors contribute to the acceleration of the leg forward in pre- and early swing (Module 5) [37].

In TFA slow walking, S1, S2, S3, and S4 correspond to Module 3, Module 2, Module 1, and Module 4 of [37], respectively. In TFA during normal walking, S2, S3, and S4 corresponded to Module 2, Module 1, and Module 4 of [37], respectively. In TFA during fast walking, S1, S2, and S4 corresponded to Module 1, Module 2, and Module 4 of [37], respectively.

The difference between the literature [37] and the present study with regards to S1 (primary: Sol, TFL) during normal walking as well as S3 (primary muscle: SEM and VL) during fast walking seemed to be affected by the synergy analysis methods, task performed (steady-state vs. transient-state), number and choice of muscles included, and difference in speed. The neuromuscular modulation between muscle synergies of TFA across speeds agreed with the study conducted by [22], suggesting changes in speeds lead to the recruitment of different spinal locomotor networks.

#### 4.5. Within-Subject Comparison (Activation Coefficient Profiles)

SPM RM ANOVA analysis showed a significant difference in TFA C1, C2, and C4 across speeds. The post-hoc TFA C1 between fast-normal and fast-slow showed significant differences in ES and TSW. The muscle synergy comparison (i.e., S1 fast-normal and S1 fast-slow) showed that they were poorly correlated with  $R^2$  of 0.13 and 0, respectively. The primary muscles in TFA C1 between slow (mainly activated TFL), normal (mainly activated SOL), and fast (mainly activated RF) were different. One could suggest the significant differences in activation timing between speeds are due to the different groups of muscle recruitment, thereby each module contributing to different biomechanical subtasks (Figures 5 and 6).

Although a high correlation was observed between S2 across speeds (pair-wise speed comparison), TFA C2 (mainly activated plantarflexor) showed to be significantly different in MS, TS, and ISW between fast and normal speeds. Since the same set of muscles were recruited across speeds, the reason for the discrepancy between the speeds may be due to the higher activation and intensity required for the plantarflexor muscles of the IL to stabilize the ankle joint during the single support stance phase and generate a larger push-off in TS with increased speed. This is evident from the significant difference that occurred during fast gait as compared to normal gait (Figures 7 and 8).

TFA C4 (mainly activated TA) was found to be significantly different in MS between fast and slow-speed walking. The activation of SEM was coordinated with TA in S4 at slow walking, in which a moderate correlation (0.5) was observed compared to fast walking. The higher magnitude of the second peak in the stance phase of fast walking (the suprathreshold cluster) occurred before the second peak in slow walking. This could be due to the kinematic and kinetic demands that altered TA activation timing (Figures 10 and 11).

Interestingly, TFA C3 showed no significant differences between speeds. The same group of muscles (SEM and VL) is associated with S3 across speeds, except at fast speeds. Observing the mean difference  $t$ -trajectory, one could observe that the black line at the end of the swing phase is very close to the critical threshold (Figure 9). The results indicate no adaptation strategy is required to augment the intensity of the temporal component.

The result of C3 was supported by the fact that the effect of speeds on the high-dimensional sEMG activity of SEM showed no significant differences, suggesting the low-dimensional and high-dimensional temporal components would be the same for this muscle (Figure 12).

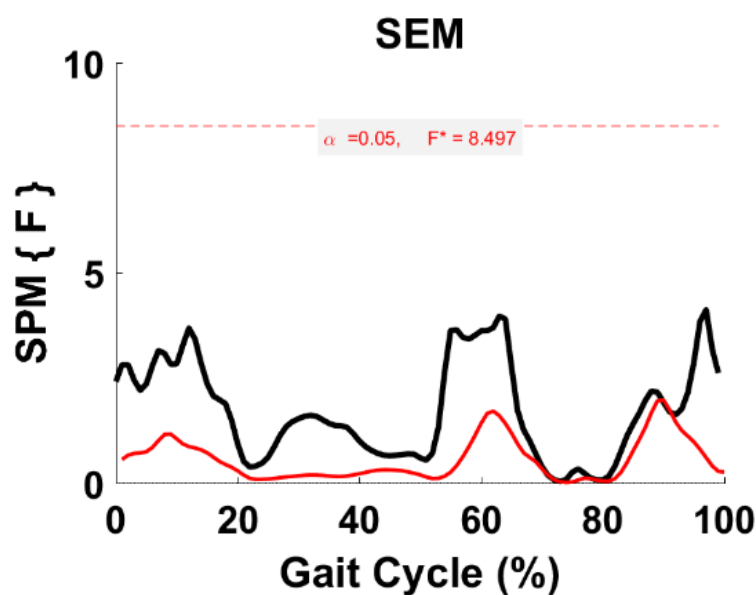


**Figure 12.** TFA SEM parametric RM ANOVA within- and between-subjects, depicting significant differences between speeds. The horizontal red dotted line indicates the critical threshold of 8.497. Suprathreshold clusters are shown in gray where  $p < 0.05$ . Black line is RM ANOVA (Within) and red line is ANOVA (Between).

#### 4.6. Comparison of the Activation Coefficient Profile with Literature

The results of the present study appear to conflict with the previous reports, as they suggested a small increase in activation coefficient timing at different walking speeds [12–14,37]. It is worth mentioning that none of the studies conducted on muscle synergies considered the whole time series as a means of comparison (i.e., using 1D SPM). This could be attributed to the fact that discrete points in traditional statistical analysis (i.e., scalar) may result in a different interpretation. Therefore, one should consider the time-normalized C waveforms, especially when there is no a priori hypothesis pertaining to the

point of interest [45,49]. In addition, the present study did not consider steady-state walking as opposed to the studies conducted in the literature [4,13,14,16,17,30–32,36–39,42,50]. In summary, the difference could be attributed to the difference in muscle synergy methodological consideration, state of walking (steady-state vs. transient-state), level of amputation, number and choice of muscles included, and the difference in speed.

#### 4.7. Potential Rehabilitative and Assistive Applications

One of the primary benefits of this study lies in its potential to enhance our comprehension of how the CNS acclimates to variations in velocity during transient-states. This understanding holds significant value in identifying effective approaches to mitigate the occurrence of trips or falls [51]. This study can potentially provide insights for therapists regarding the muscle coordination patterns adopted by lower limb amputees during unsteady gait conditions. Additionally, it can contribute to the development of rehabilitation programs that effectively enhance the balance and mobility of individuals with amputations. Furthermore, the findings of this study have the potential to assist prosthetic companies in the development of a myoelectric prosthetic system capable of detecting and responding to trips or falls during various phases of human locomotion.

#### 4.8. Limitations

Limiting muscle synergy analysis to only male participants among transfemoral amputees poses a significant limitation in terms of the generalizability and applicability of the findings. Gender differences in muscle composition, biomechanics, and neuromuscular control could influence the observed synergies. Researchers should strive for a more representative sample to ensure that the outcomes are relevant and applicable across different demographic groups within the transfemoral amputee population.

Only ten muscles have been included in this study for the TFA. In the literature, the number varies from 8 to 31 muscles during gait [13,16,52]. As reported by [52], the number of muscles has an impact on the neuromuscular results. Therefore, the results may have varied if more muscles were included in the study. Only superficial muscles were included in the present study. Prior research focused on the effect of deeper muscles during activities of daily living. However, it has been shown that the number of synergies is invariant when compared to synergies extracted only from superficial muscles [16]. Finally, a larger pool of homogenous amputees with a similar prosthesis is required to be able to generalize the results of this study.

The methodology implemented in this paper was based on global muscle synergy analysis (i.e., time domain), in which the linear envelope of signals was input to the algorithm. Another approach to investigating the neuro-structure underlying muscle activation is to extract spectral properties (i.e., time-frequency domain). This has been proposed by Frere [36] to distinguish between descriptive and prescriptive analysis.

### 5. Summary

Overall, these results provide valuable insights into the adaptations and differences in muscle synergies and their activations across different walking speeds in transfemoral amputees. The findings highlight the importance of considering specific muscle groups and their activation timing in relation to biomechanical subtasks during gait. The discrepancies observed between speeds demonstrate the adaptability and specific demands placed on different muscle groups. These insights can inform the development of rehabilitation strategies and prosthetic interventions aimed at optimizing gait performance in transfemoral amputees.

### 6. Conclusions

TFA illustrated that four synergies are an optimal number of groups to match the reconstructed and original EMG at all speeds. This suggests that the complexity of muscle recruitment by the CNS is analogous in TFA and non-amputees. Therefore, there is no

compensatory adjustment in TFA. The low correlation between TFA muscle synergies across speeds could be attributed to the significant change in speeds that resulted in neuromuscular modulations at the transition from stance to swing phase and body support phase of the GC. The effect of speeds on individual activation coefficient profiles of TFA showed significant differences (except TFA C3), indicating the CNS strategy to increase the intensity of the activation coefficient profile to satisfy the kinematic and kinetic requirements of different speeds. No significant differences were found in TFA C3, suggesting no adaptation strategy is required to augment the intensity of the temporal component.

**Supplementary Materials:** The following supporting information can be downloaded at: <https://www.mdpi.com/article/10.3390/biomechanics4010002/s1>; Table S1: Average of each participant's slow walking trials during the transient-state; Figure S1: The probability density of TFA slow speed; Figure S2: The green bars depict the observed distribution speed and the black curve represents the fitted normal distribution for TFA slow speed. Table S2: Average of each participant's normal walking speed during the transient-state; Figure S3: The probability density of TFA normal speed; Figure S4: The blue bars depict the observed distribution speed and the black curve represents the fitted normal distribution for TFA normal speed; Table S3. Average of each participant's fast walking speed during the transient-state; Figure S5: The probability density of TFA fast speed; Figure S6: The red bars depict the observed distribution speed and the black curve represents the fitted normal distribution for TFA fast speed.

**Author Contributions:** Conceptualization, P.M., M.S. and T.R.; methodology, P.M., M.S., T.R. and A.K.; software, P.M.; validation and formal analysis, P.M., M.S. and T.R.; resources, N.M., F.F., R.O. and A.D.-S.; data curation, P.M., T.R. and A.K.; writing—original draft preparation, P.M.; writing—review and editing, all authors; supervision, N.M., F.F., R.O. and A.D.-S.; project administration, A.D.-S. All authors have read and agreed to the published version of the manuscript.

**Funding:** This research received no external funding.

**Institutional Review Board Statement:** This study was conducted in accordance with the Declaration of Helsinki and approved by the Ethical Review Boards (or Ethics Committee) at the Djavad Mowafaghian Research Centre of Intelligent Neuro-Rehabilitation Technologies in Tehran, Iran, and the University of Leeds in the UK, which approved the experimental protocol (approved in November 2017; approval code: SUT-926744).

**Informed Consent Statement:** Informed consent was obtained from all subjects involved in this study.

**Data Availability Statement:** The data presented in this study are available on request from the corresponding author. The data are not publicly available due to privacy and ethical restrictions.

**Acknowledgments:** The present study was supported academically by the Sharif University of Technology and the University of Leeds. The authors appreciate all participants' involvement in this study and the assistance of Farzam Farahmand, the "Djavad Mowafaghian Research Centre of Intelligent Neuro-Rehabilitation Technologies", and Zahra Rafiei, manager of its Gait Lab.

**Conflicts of Interest:** The authors declare no conflicts of interest.

## References

1. Cappellini, G.; Ivanenko, Y.P.; Poppele, R.E.; Lacquaniti, F. Motor patterns in human walking and running. *J. Neurophysiol.* **2006**, *95*, 3426–3437. [[CrossRef](#)]
2. Mehryar, P.; Shourijeh, M.S.; Rezaeian, T.; Khandan, A.R.; Messenger, N.; O'Connor, R.; Farahmand, F.; Dehghani-Sanij, A. Muscular activity comparison between non-amputees and transfemoral amputees during normal transient-state walking speed. *Med. Eng. Phys.* **2021**, *95*, 39–44. [[CrossRef](#)] [[PubMed](#)]
3. Mehryar, P.; Rezaeian, T.; Shourijeh, M.S.; Raveendranathan, V.; Messenger, N.; O'Connor, R.; Dehghani-Sanij, A. Changes in knee joint kinetics of transfemoral amputee's intact leg: An osteoarthritis indication? *Gait Posture* **2017**, *57*, 151–152. [[CrossRef](#)]
4. Mehryar, P.; Shourijeh, M.S.; Rezaeian, T.; Khandan, A.R.; Messenger, N.; O'Connor, R.; Farahmand, F.; Dehghani-Sanij, A. Differences in muscle synergies between healthy subjects and transfemoral amputees during normal transient-state walking speed. *Gait Posture* **2020**, *76*, 98–103. [[CrossRef](#)] [[PubMed](#)]
5. De Marchis, C.; Ranaldi, S.; Serrao, M.; Ranavolo, A.; Draicchio, F.; Lacquaniti, F.; Conforto, S. Modular motor control of the sound limb in gait of people with trans-femoral amputation. *J. Neuroeng. Rehabil.* **2019**, *16*, 132. [[CrossRef](#)] [[PubMed](#)]

6. Tokuno, C.D.; Sanderson, D.J.; Inglis, J.T.; Chua, R. Postural and movement adaptations by individuals with a unilateral below-knee amputation during gait initiation. *Gait Posture* **2003**, *18*, 158–169. [[CrossRef](#)] [[PubMed](#)]
7. Park, S.; Choi, H.; Ryu, K.; Kim, S.; Kim, Y. Kinematics, kinetics and muscle activities of the lower extremity during the first four steps from gait initiation to the steady-state walking. *J. Mech. Sci. Technol.* **2009**, *23*, 204–211. [[CrossRef](#)]
8. Mehryar, P. High Dimensional Surface Electromyography and Low Dimensional Muscle Synergy in Lower Limb Amputees during Transient-and Steady-State Gait. Doctoral Thesis, University of Leeds, Leeds, UK, 2018.
9. Mbourou, G.A.; Lajoie, Y.; Teasdale, N. Step length variability at gait initiation in elderly fallers and non-fallers, and young adults. *Gerontology* **2003**, *49*, 21–26. [[CrossRef](#)]
10. Wong, C.K.; Chihuri, S.T.; Li, G. Risk of fall-related injury in people with lower limb amputations: A prospective cohort study. *J. Rehabil. Med.* **2016**, *48*, 80–85. [[CrossRef](#)]
11. Vanicek, N.; Strike, S.; McNaughton, L.; Polman, R. Gait patterns in transtibial amputee fallers vs. non-fallers: Biomechanical differences during level walking. *Gait Posture* **2009**, *29*, 415–420. [[CrossRef](#)] [[PubMed](#)]
12. Gonzalez-Vargas, J.; Sartori, M.; Dosen, S.; Torricelli, D.; Pons, J.L.; Farina, D. A predictive model of muscle excitations based on muscle modularity for a large repertoire of human locomotion conditions. *Front. Comput. Neurosci.* **2015**, *9*, 114. [[CrossRef](#)]
13. Clark, D.J.; Ting, L.H.; Zajac, F.E.; Neptune, R.R.; Kautz, S.A. Merging of healthy motor modules predicts reduced locomotor performance and muscle coordination complexity post-stroke. *J. Neurophysiol.* **2009**, *103*, 844–857. [[CrossRef](#)]
14. Gui, K.; Zhang, D. Influence of locomotion speed on biomechanical subtask and muscle synergy. *J. Electromyogr. Kinesiol.* **2016**, *30*, 209–215. [[CrossRef](#)]
15. Ivanenko, Y.; Cappellini, G.; Poppele, R.; Lacquaniti, F. Spatiotemporal organization of  $\alpha$ -motoneuron activity in the human spinal cord during different gaits and gait transitions. *Eur. J. Neurosci.* **2008**, *27*, 3351–3368. [[CrossRef](#)] [[PubMed](#)]
16. Saito, A.; Tomita, A.; Ando, R.; Watanabe, K.; Akima, H. Similarity of muscle synergies extracted from the lower limb including the deep muscles between level and uphill treadmill walking. *Gait Posture* **2018**, *59*, 134–139. [[CrossRef](#)]
17. Hagio, S.; Fukuda, M.; Kouzaki, M. Identification of muscle synergies associated with gait transition in humans. *Front. Hum. Neurosci.* **2015**, *9*, 48. [[CrossRef](#)] [[PubMed](#)]
18. Ivanenko, Y.P.; Poppele, R.E.; Lacquaniti, F. Five basic muscle activation patterns account for muscle activity during human locomotion. *J. Physiol.* **2004**, *556*, 267–282. [[CrossRef](#)]
19. McGowan, C.P.; Neptune, R.R.; Clark, D.J.; Kautz, S.A. Modular control of human walking: Adaptations to altered mechanical demands. *J. Biomech.* **2010**, *43*, 412–419. [[CrossRef](#)] [[PubMed](#)]
20. Lacquaniti, F.; Ivanenko, Y.P.; Zago, M. Patterned control of human locomotion. *J. Physiol.* **2012**, *590*, 2189–2199. [[CrossRef](#)]
21. Kibushi, B.; Hagio, S.; Moritani, T.; Kouzaki, M. Speed-dependent modulation of muscle activity based on muscle synergies during treadmill walking. *Front. Hum. Neurosci.* **2018**, *12*, 4. [[CrossRef](#)] [[PubMed](#)]
22. Yokoyama, H.; Ogawa, T.; Kawashima, N.; Shinya, M.; Nakazawa, K. Distinct sets of locomotor modules control the speed and modes of human locomotion. *Sci. Rep.* **2016**, *6*, 36275. [[CrossRef](#)]
23. Rodriguez, K.L.; Roemmich, R.T.; Cam, B.; Fregly, B.J.; Hass, C.J. Persons with Parkinson’s disease exhibit decreased neuromuscular complexity during gait. *Clin. Neurophysiol.* **2013**, *124*, 1390–1397. [[CrossRef](#)] [[PubMed](#)]
24. Danner, S.M.; Hofstoetter, U.S.; Freundl, B.; Binder, H.; Mayr, W.; Rattay, F.; Minassian, K. Human spinal locomotor control is based on flexibly organized burst generators. *Brain* **2015**, *138*, 577–588. [[CrossRef](#)] [[PubMed](#)]
25. Steele, K.M.; Rozumalski, A.; Schwartz, M.H. Muscle synergies and complexity of neuromuscular control during gait in cerebral palsy. *Dev. Med. Child Neurol.* **2015**, *57*, 1176–1182. [[CrossRef](#)] [[PubMed](#)]
26. Routson, R.L.; Clark, D.J.; Bowden, M.G.; Kautz, S.A.; Neptune, R.R. The influence of locomotor rehabilitation on module quality and post-stroke hemiparetic walking performance. *Gait Posture* **2013**, *38*, 511–517. [[CrossRef](#)]
27. Cheung, V.C.; Turolla, A.; Agostini, M.; Silvoni, S.; Bennis, C.; Kasi, P.; Paganoni, S.; Bonato, P.; Bizzi, E. Muscle synergy patterns as physiological markers of motor cortical damage. *Proc. Natl. Acad. Sci. USA* **2012**, *109*, 14652–14656. [[CrossRef](#)]
28. Hayes, H.B.; Chvatal, S.A.; French, M.A.; Ting, L.H.; Trumbower, R.D. Neuromuscular constraints on muscle coordination during overground walking in persons with chronic incomplete spinal cord injury. *Clin. Neurophysiol.* **2014**, *125*, 2024–2035. [[CrossRef](#)] [[PubMed](#)]
29. Roh, J.; Rymer, W.Z.; Perreault, E.J.; Yoo, S.B.; Beer, R.F. Alterations in upper limb muscle synergy structure in chronic stroke survivors. *J. Neurophysiol.* **2013**, *109*, 768–781. [[CrossRef](#)]
30. Gizzi, L.; Nielsen, J.F.; Felici, F.; Ivanenko, Y.P.; Farina, D. Impulses of activation but not motor modules are preserved in the locomotion of subacute stroke patients. *J. Neurophysiol.* **2011**, *106*, 202–210. [[CrossRef](#)]
31. Mehryar, P.; Shourijeh, M.; Rezaeian, T.; Iqbal, N.; Messenger, N.; Dehghani-Sanij, A.A. Changes in synergy of transtibial amputee during gait: A pilot study. In *Biomedical & Health Informatics (BHI), Proceedings of the 2017 IEEE EMBS International Conference, Orlando, FL, USA, 16–19 February 2017*; IEEE: Piscataway, NJ, USA, 2017; pp. 325–328.
32. Mehryar, P.; Shourijeh, M.; Maqbool, H.F.; Torabi, M.; Dehghani-Sanij, A.A. Muscle synergy analysis in transtibial amputee during ramp ascending activity. In *Engineering in Medicine and Biology Society (EMBC), Proceedings of the 2016 IEEE 38th Annual International Conference, Orlando, FL, USA, 16–20 August 2016*; IEEE: Piscataway, NJ, USA, 2016; pp. 1676–1679.
33. Mehryar, P.; Shourijeh, M.S.; Dehghani-Sanij, A.A. *Muscle Synergy Analysis in Transtibial Amputee during Ramp Descending Activity*; Springer International Publishing: Cham, Switzerland, 2017; pp. 945–950.

34. Bus, S.A.; de Lange, A. A comparison of the 1-step, 2-step, and 3-step protocols for obtaining barefoot plantar pressure data in the diabetic neuropathic foot. *Clin. Biomech.* **2005**, *20*, 892–899. [[CrossRef](#)]
35. Stegeman, D.; Hermens, H. Standards for surface electromyography: The European project Surface EMG for non-invasive assessment of muscles (SENIAM). *Enschede Roessingh Res. Dev.* **2007**, *10*, 108–112.
36. Frère, J. Spectral properties of multiple myoelectric signals: New insights into the neural origin of muscle synergies. *Neuroscience* **2017**, *355*, 22–35. [[CrossRef](#)]
37. Neptune, R.R.; Clark, D.J.; Kautz, S.A. Modular control of human walking: A simulation study. *J. Biomech.* **2009**, *42*, 1282–1287. [[CrossRef](#)]
38. Oliveira, A.S.; Gizzi, L.; Farina, D.; Kersting, U.G. Motor modules of human locomotion: Influence of EMG averaging, concatenation, and number of step cycles. *Front. Hum. Neurosci.* **2014**, *8*, 335. [[CrossRef](#)] [[PubMed](#)]
39. Serrancolí, G.; Monllau, J.C.; Font-Llagunes, J.M. Analysis of muscle synergies and activation–deactivation patterns in subjects with anterior cruciate ligament deficiency during walking. *Clin. Biomech.* **2016**, *31*, 65–73. [[CrossRef](#)]
40. Shourijeh, M.S.; Flaxman, T.E.; Benoit, D.L. An approach for improving repeatability and reliability of non-negative matrix factorization for muscle synergy analysis. *J. Electromyogr. Kinesiol.* **2016**, *26*, 36–43. [[CrossRef](#)] [[PubMed](#)]
41. Torres-Oviedo, G.; Macpherson, J.M.; Ting, L.H. Muscle synergy organization is robust across a variety of postural perturbations. *J. Neurophysiol.* **2006**, *96*, 1530–1546. [[CrossRef](#)] [[PubMed](#)]
42. Sartori, M.; Gizzi, L.; Lloyd, D.G.; Farina, D. A musculoskeletal model of human locomotion driven by a low dimensional set of impulsive excitation primitives. *Front. Comput. Neurosci.* **2013**, *7*, 79. [[CrossRef](#)]
43. Torres-Oviedo, G.; Ting, L.H. Muscle synergies characterizing human postural responses. *J. Neurophysiol.* **2007**, *98*, 2144–2156. [[CrossRef](#)]
44. Portney, L.; Watkins, M. *Foundations of Clinical Research: Application to Practice*; Appleton & Lange: Stamford, CT, USA, 1993.
45. Pataky, T.C.; Robinson, M.A.; Vanrenterghem, J. Vector field statistical analysis of kinematic and force trajectories. *J. Biomech.* **2013**, *46*, 2394–2401. [[CrossRef](#)]
46. Guidetti, L.; Rivellini, G.; Figura, F. EMG patterns during running: Intra-and inter-individual variability. *J. Electromyogr. Kinesiol.* **1996**, *6*, 37–48. [[CrossRef](#)] [[PubMed](#)]
47. Hug, F. Can muscle coordination be precisely studied by surface electromyography? *J. Electromyogr. Kinesiol.* **2011**, *21*, 1–12. [[CrossRef](#)] [[PubMed](#)]
48. Miall, R.C. Walking the walk. *Nat. Neurosci.* **2007**, *10*, 940. [[CrossRef](#)] [[PubMed](#)]
49. Robinson, M.A.; Vanrenterghem, J.; Pataky, T.C. Statistical Parametric Mapping (SPM) for alpha-based statistical analyses of multi-muscle EMG time-series. *J. Electromyogr. Kinesiol.* **2015**, *25*, 14–19. [[CrossRef](#)] [[PubMed](#)]
50. De Groote, F.; Jonkers, I.; Duysens, J. Task constraints and minimization of muscle effort result in a small number of muscle synergies during gait. *Front. Comput. Neurosci.* **2014**, *8*, 115. [[CrossRef](#)]
51. Abd, A.T.; Singh, R.E.; Iqbal, K.; White, G. A Perspective on Muscle Synergies and Different Theories Related to Their Adaptation. *Biomechanics* **2021**, *1*, 253–263. [[CrossRef](#)]
52. Steele, K.M.; Tresch, M.C.; Perreault, E.J. The number and choice of muscles impact the results of muscle synergy analyses. *Front. Comput. Neurosci.* **2013**, *7*, 105. [[CrossRef](#)]

**Disclaimer/Publisher’s Note:** The statements, opinions and data contained in all publications are solely those of the individual author(s) and contributor(s) and not of MDPI and/or the editor(s). MDPI and/or the editor(s) disclaim responsibility for any injury to people or property resulting from any ideas, methods, instructions or products referred to in the content.